

A Novel NOMA Solution with RIS Partitioning

Aymen Khaleel, *Student Member, IEEE* and Ertugrul Basar, *Senior Member, IEEE*

Abstract—Reconfigurable intelligent surface (RIS) empowered communications with non-orthogonal multiple access (NOMA) has recently become as an appealing research direction for the next-generation wireless communications. In this paper, we propose a novel NOMA solution with RIS partitioning, where we aim to enhance the spectrum efficiency by improving the ergodic rate of all users, and to maximize the user fairness. In the proposed system, we distribute the physical resources among users such that the base station (BS) and RIS are dedicated to serve different clusters of users. Furthermore, we formulate an RIS partitioning optimization problem to slice the RIS elements between the users such that the user fairness is maximized. The formulated problem is a non-convex and non-linear integer programming (NLIP) problem with a combinatorial feasible set, which is very challenging to solve. Therefore, we exploit the structure of the problem to bound its feasible set and obtain a sub-optimal solution by sequentially applying three efficient search algorithms. Furthermore, we derive exact and asymptotic expressions for the outage probability. Simulation results clearly indicate the superiority of the proposed system over the considered benchmark systems in terms of ergodic sum-rate, outage probability, and user fairness performance.

Index Terms—Reconfigurable intelligent surface (RIS), non-orthogonal multiple access (NOMA), user fairness, sum-rate.

I. INTRODUCTION

NON-ORTHOGONAL multiple access (NOMA) has been regarded as one of the promising technologies to address the increasing demand for high data rates, massive connectivity, and spectrum efficiency associated with fifth-generation (5G) and beyond networks. This is because NOMA allows the sharing of the same time/frequency/code resources between users and thus, enhances the spectrum efficiency and decreases the latency by allowing more users to be connected in the same time slot [1]. In power domain (PD)-NOMA [2], the difference in channel gains of different users is exploited and, accordingly, different power levels are assigned to different users by the use of superposition coding (SC) at the base station (BS) side. At the receiver side, each user employs the successive interference cancellation (SIC) technique to recover its own message. Compared to the orthogonal multiple access (OMA), it has been shown that NOMA has a superior performance in terms of the outage probability and the ergodic sum-rate [3], [4].

Recently, reconfigurable intelligent surface (RIS)-assisted communication has received growing attention as a potential next-generation technology due to its promising capabilities to control the wireless propagation environment. RIS is an array of low-cost and passive reflecting elements that can be used to re-engineer the electromagnetic waves by adjusting

the reflection coefficient of each element [5], [6]. Due to their promising advantages, RISs have been integrated to many of the existing wireless technologies as a main or supportive module in the communications system. In [7], an RIS is integrated to a conventional single-input single-output (SISO) system to achieve an ultra-reliable communication system. In [8], an RIS is used as a part of the transmitter to perform different types of index modulation (IM) and thus, obviating the need for a multi-antenna BS. These techniques are extended to multiple-input multiple-output (MIMO) systems in [9], where an RIS is used to replace the radio frequency (RF) chain in Alamouti's scheme, and to boost the data rate for vertical Bell Labs layered space-time (VBLAST) system by using IM.

Recently, the joint operation of RISs with NOMA has appeared as an appealing research direction and the combination of the hardware capabilities of RISs and the SC technique of PD-NOMA has been investigated. In [10] and [11], the rate performance and user fairness of an RIS-assisted NOMA system are optimized by maximizing the minimum decoding signal-to-interference-plus-noise ratio (SINR) of all users, which is achieved by the joint optimization of the active and passive beamforming at the BS and the RIS, respectively. The authors in [12] considered an RIS-assisted multiple-input single-output (MISO) NOMA system where the cell-center users are served by using spatial division multiple access (SDMA) and the cell-edge users are served by RISs. In [13], by considering a priority-oriented design, an RIS-assisted SISO NOMA network is proposed, where the passive beamforming weights are designed at the RIS side in order to enhance the spectrum efficiency. In [14], the energy efficiency is enhanced in a downlink RIS-assisted NOMA system by jointly optimizing the user clustering, passive beamforming, and power allocation. The user fairness is considered in [15], where the authors investigated the joint optimization of power allocation, decoding order, and the RIS phase shifts to maximize the minimum user rate considering a total power constraint. In [16], the deployment and passive beamforming design of an RIS are investigated for an RIS-assisted MISO NOMA system, in order to maximize the energy efficiency under the constraint of preserving the individual data rate requirements for users. Joint optimization for the active beamforming matrices at the BS and the reflection coefficient vector at the RIS is utilized in [17] in order to minimize the total transmit power for a multi-cluster MISO NOMA networks. In [18], a multi-cluster RIS-assisted MIMO NOMA network is considered, where by designing its passive beamforming weights, the RIS is employed in a signal cancellation mode to eliminate the inter-cluster interference. The authors in [19] and [20] used stochastic geometry to investigate the coverage probability and ergodic rate of an RIS-assisted multi-cell NOMA networks for outdoor scenarios by

The authors are with the Communications Research and Innovation Laboratory (CoreLab), Department of Electrical and Electronics Engineering, Koç University, Sariyer 36050, Istanbul, Turkey. Email: akhaleel18@ku.edu.tr, ebasar@ku.edu.tr

using Poisson cluster process (PCP) model. The authors in [21] considered the combination of joint transmission coordinated multipoint (JT-CoMP) with the RIS technology in order to enhance the cell-edge user ergodic rate performance without degrading the performance of the cell-center user. In [22], the authors investigated the impact of the coherent and the random discrete phase-shifting designs on an RIS-assisted NOMA system. Finally, the authors in [23] considered the resource allocation problem in an RIS-assisted NOMA system, they jointly optimized the channel assignments, power allocation, decoding order, and RIS reflection coefficients, in order to maximize the system throughput.

In light of these, it can be noted that there is a common approach followed by all of the previous works, which can be summarized as follows. The BS and RIS are both used to serve all users by using a single SC message. Furthermore, by adjusting its reflection coefficients, the RIS is used as a single unit to serve all users. Considering this followed approach, the main factor that limits the users' performance becomes the mutual interference that underlies the SC technique. Although the fact that the RIS enhances all users' signal-to-noise ratio (SNR) by amplifying the SC message, low signal-to-interference ratio (SIR) values still raise a concern. Therefore, the use of SC to combine the symbols of all users in a single message can significantly limit the obtainable gain from the RIS.

Against this background, we propose an RIS-assisted novel NOMA system, where we aim to improve all users' performance in terms of ergodic rate, outage probability, and user fairness. In the proposed system, the users are grouped into two clusters, Cluster 1 (C_1) which contains all the users located out the field-of-view (FoV) of the RIS, and Cluster 2 (C_2) that contains the ones located in the FoV of the RIS. Based on the locations of the users' clusters, the physical resources (BS and RIS) are distributed fairly among users, where the BS and RIS are dedicated to serve C_1 and C_2 , respectively. Instead of considering it as a single unit, the RIS is partitioned into sub-surfaces, where each sub-surface is exploited to serve a different user. In order to maximize user fairness among the users served by the RIS, an RIS partitioning optimization problem is formulated and three efficient search algorithms are proposed to solve it by finding the optimum RIS split. Furthermore, instead of combining all users' symbols in a single SC message, the transmission of C_1 and C_2 users' symbols is simultaneously performed over two stages. In the first stage, C_1 users' symbols are transmitted from the BS using SC, while C_2 users' symbols are transmitted by using the RIS in the second stage. By considering this transmission mechanism, the mutual interference between users is effectively mitigated and thus, the detection process of symbols is significantly simplified for all users. The main contributions of this paper can be summarized as follows:

- We propose a novel NOMA solution with RIS partitioning that aims interference-mitigated transmission, fair distribution to the physical resources among users, and simplifies the detection process for all users.
- We formulate an RIS partitioning optimization problem to find a proper RIS slicing that maximizes the fairness among

C_2 users. Although the fact that the formulated problem is a non-convex and non-linear integer programming (NLIP) one, we exploit the structure of the problem, specifically the nature of transmission over the RIS, to provide a sub-optimal solution with marginal performance degradation.

- We derive the exact and asymptotic outage probability expressions for users in C_2 .
- With comprehensive computer simulations, we compare our proposed system with three different benchmark schemes and show the superiority of our proposed system in terms of the ergodic sum-rate, outage probability, and user fairness.

The rest of the paper is organized as follows. In Section II, we introduce the system model and describe the transmission mechanism in detail. The outage probability and its asymptotic behaviour are formulated in Section III. In Section IV, we introduce our proposed RIS partitioning approach and provide the system performance analysis of two special cases for the proposed system in different deployment scenarios. Computer simulations are provided in Section V followed by the conclusions in Section VI.

II. RIS PARTITIONING AND ROTATING: SYSTEM MODEL

Consider a downlink NOMA system where single-antenna users are served by a single-antenna BS and an RIS with N elements. The users are assumed to be grouped into two clusters, C_1 with M_1 users and C_2 with M_2 users, as shown in Fig. 1. The RIS is deployed close, yet in the far-field, to the BS in order to exploit the pure line-of-sight (LOS) channels and to make the use of a feedback link from the BS to the RIS practical. Furthermore, denoting the m^{th} user in C_2 by $U_{m,2}$, perfect channel state information (CSI) of the BS-RIS- $U_{m,2}$ link for all users in C_2 needs to be available at the RIS side. On the other hand, the channel gains of all users in C_1 need to be available at the BS side. Instead of combining the symbols of all users in a single SC message transmitted from the BS, the transmission of C_1 and C_2 users' symbols is simultaneously performed over two stages, as follows. In the first stage, as in PD-NOMA, SC is used to superpose the symbols belong to C_1 users in a single message transmitted from the BS. In the second stage, each sub-surface of the RIS acts as a transmitter to a specific user in C_2 by manipulating the signals that imping its elements to reflect the pure symbol of that specific user. In what follows, we describe these two stages of transmission in detail.

Considering the first stage of transmission, as in conventional PD-NOMA, the BS transmits x , which is the superposed signal of all symbols to be transmitted to the M_1 users in C_1 . Here $x = ue^{j\theta_{M_1}}$, where u and $\theta_{M_1} \in [0, 2\pi]$ are the amplitude and phase of x , respectively, and x is constructed as follows:

$$x = \sum_{m=1}^{M_1} \sqrt{P\zeta_m} x_m, \quad (1)$$

where P is the transmit power, ζ_m and x_m are the power allocation factor and the symbol to be transmitted to user m in C_1 ($U_{m,1}$), respectively, where $\sum_{m=1}^{M_1} \zeta_m = 1$. Thus, the signal received by each user m in C_1 is given by

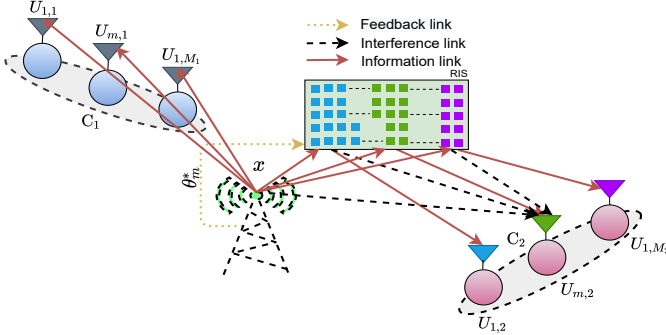


Fig. 1. RIS partitioning based NOMA system.

$$\tilde{y}_m = \tilde{v}_m x + \tilde{z}_m, \quad (2)$$

where \tilde{v}_m is the BS- $U_{m,1}$ channel coefficient and \tilde{z}_m is the additive white Gaussian noise (AWGN) sample at $U_{m,1}$. From (2), it can be noted that there is no interference from C_2 users' symbols received by C_1 users. Although C_1 users still need to use SIC to recover their own signals, the SIC is performed with significantly less number of iterations due to the absence of C_2 users' interference. This simplifies the detection process and effectively reduces the error propagation associated with the SIC technique. In this way, the system performance for the M_1 users in C_1 follows the one of the conventional PD-NOMA and, therefore, its analysis is omitted in this study.

Considering the second stage of transmission, in order to serve the users in C_2 , the RIS is partitioned into M_2 sub-surfaces, where each sub-surface i has N_i elements and is allocated to a specific user m in C_2 , for $i = m$, where $m = 1, 2, \dots, M_2$. By properly and independently adjusting its phase shifts, each sub-surface $i = m$ performs two roles, namely, maximizing the channel gain by making the BS-RIS- $U_{m,2}$ channel phases equal to zero, and rotating x to reflect the phase shift keying (PSK) symbol to be transmitted to $U_{m,2}$. Note that, due to the SC process of the symbols of C_1 users, the amplitude and phase of x are both, generally, random variables. Nevertheless, since the symbols sent to C_2 users are PSK symbols, the phase of x is the only parameter that needs to be considered at the RIS to perform the rotation process. Thus, by considering only single reflections from the RIS [24], the signal received by each user m in C_2 can be obtained as follows:

$$y_m = \left[\mathbf{g}_{m,m}^T \mathbf{\Theta}_m \mathbf{h}_m + \sum_{i \neq m}^{M_2-1} \mathbf{g}_{i,m}^T \mathbf{\Theta}_i \mathbf{h}_i + v_m \right] x + z_m, \quad (3)$$

where $z_m \sim \mathcal{CN}(0, \sigma^2)$ is the AWGN sample at $U_{m,2}$, and $\mathcal{CN}(0, \sigma^2)$ stands for complex Gaussian distribution with zero mean and σ^2 variance. v_m is the BS- $U_{m,2}$ channel coefficient, $v_m \sim \mathcal{CN}(0, L_m^{\text{BS}})$, under Rayleigh fading assumption, where L_m^{BS} denotes the BS- $U_{m,2}$ path gain. $\mathbf{h}_i = [\sqrt{L_m^{\text{RIS}h}} e^{-j\psi^{(1)}}, \dots, \sqrt{L_m^{\text{RIS}h}} e^{-j\psi^{(n)}}, \dots, \sqrt{L_m^{\text{RIS}h}} e^{-j\psi^{(N_i)}}]$ is the BS- $(i^{\text{th}}$ sub-surface) channel vector, assuming pure LOS links, $\psi^{(n)} \in [0, 2\pi]$ is the phase shift $\frac{2\pi a_n}{\lambda}$ associated with the LOS link [25], λ is the wavelength for the given operating frequency, $L_m^{\text{RIS}h}$ and a_n denote the BS-RIS (i^{th} sub-surface n^{th} element) path gain and distance,

respectively. Since the RIS is deployed in the far-field of the BS, the path gain experienced by each element is assumed to be the same, where the spacing between the elements is small compared to the BS-RIS distance. $\mathbf{g}_{i,m} = [\sqrt{L_m^{\text{RIS}g}} g_{i,m}^{(1)}, \dots, \sqrt{L_m^{\text{RIS}g}} g_{i,m}^{(n)}, \dots, \sqrt{L_m^{\text{RIS}g}} g_{i,m}^{(N_i)}]$ is the RIS (i^{th} sub-surface)- $U_{m,2}$ channel vector, where $g_{i,m}^{(n)}$ and $L_m^{\text{RIS}g}$ are the RIS (i^{th} sub-surface n^{th} element)- $U_{m,2}$ small-scale fading coefficient and path gain, respectively. $g_{i,m}^{(n)} = \beta_{i,m}^{(n)} e^{-j\phi_{i,m}^{(n)}}$ where $\beta_{i,m}^{(n)}$ and $\phi_{i,m}^{(n)}$ denote the channel amplitude and phase, respectively, $g_{i,m}^{(n)} \sim \mathcal{CN}(0, 1), \forall i, m, n$. $\mathbf{\Theta}_i = \text{diag}([\eta_i^{(1)} e^{j\Phi_i^{(1)}}, \dots, \eta_i^{(n)} e^{j\Phi_i^{(n)}}, \dots, \eta_i^{(N_i)} e^{j\Phi_i^{(N_i)}}])$ is the matrix of reflection coefficients for the i^{th} sub-surface of the RIS, where $\Phi_i^{(n)} \in [0, 2\pi)$ and $\eta_i^{(n)} = 1, \forall i, n$, assuming full reflection.

Furthermore, in order to rotate x and convey the virtual PSK symbol of the m^{th} user in C_2 , the RIS (m^{th} sub-surface) phases are adjusted such that the phase of each element is given as

$$\Phi_m^{(n)} = \phi_{m,m}^{(n)} + \psi^{(n)} + \theta_m^*, \quad (4)$$

where $\theta_m^* \in [0, 2\pi]$ is the rotation phase which is assumed to be sent from the BS to the RIS (for all M_2 users) using the feedback link, and it is given by

$$\theta_m^* = \theta_m - \theta_{M_1}, \quad (5)$$

where $\theta_m \in [0, 2\pi]$ denotes the phase of the PSK symbol to be transmitted to $U_{m,2}$. By substituting (5) in (4), we get

$$\Phi_m^{(n)} = \phi_{m,m}^{(n)} + \psi^{(n)} + \theta_m - \theta_{M_1}. \quad (6)$$

According to this phase adjustment, in (3), the first three terms represent the amplitudes of the constructive combining, the intra-cluster, and inter-clusters interference, respectively. Note that, by considering the rotation process of x at the RIS side, there is no interference from C_1 users' symbols received by C_2 users over the RIS link. However, for each user m in C_2 , the interference coming from the other sub-surfaces ($i \neq m$) and the one comes from the BS is irremovable [26] and thus, considered as noise. Therefore, the users in C_2 perform maximum likelihood (ML) detection to detect their own symbols in the presence of interference. Nevertheless, by properly choosing the RIS size [27], each user m in C_2 relies on the amplification gain provided by its own sub-surface ($i = m$) to overcome the irremovable interference that comes from the BS and the other sub-surfaces ($i \neq m$). It is worth noting that, unlike the interference associated with the BS and the sub-surfaces, in classical RIS-assisted NOMA systems, increasing the RIS size does not affect the users' interference associated with SC. Thus, from (3), the instantaneous SINR for $U_{m,2}$ can be obtained as

$$\text{SINR}_m = \frac{|\mathbf{g}_{m,m}^T \mathbf{\Theta}_m \mathbf{h}_m x|^2}{\left| \left[\sum_{i \neq m}^{M_2-1} \mathbf{g}_{i,m}^T \mathbf{\Theta}_i \mathbf{h}_i + v_m \right] x \right|^2 + \frac{1}{\rho}}, \quad (7)$$

where $\rho = \frac{P}{\sigma^2}$ denotes the transmit SNR. From (7), we introduce A_m and I_m to represent the signal and total interference powers, respectively, as follows:

$$A_m = \left| [\mathbf{g}_{m,m}^T \mathbf{\Theta}_m \mathbf{h}_m] u e^{i\theta_{M_1}} \right|^2, \quad (8)$$

$$I_m = \left| \left[\sum_{i=1}^{M_2-1} \mathbf{g}_{i,m}^T \mathbf{\Theta}_i \mathbf{h}_i + v_m \right] u e^{i\theta_{M_1}} \right|^2, \quad (9)$$

without loss of generality, in order to simplify our derivations, u is assumed to be a constant value that is equal to unity, which can be achieved by the proper design of the constellations used to obtain x_1 and x_2 for C_1 users [28], [29]. For example, consider the simple case of two users in C_1 , where $x_1 \in \{\frac{t}{\sqrt{2}}(1+1j), \frac{t}{\sqrt{2}}(-1-1j)\}$ and $x_2 \in \{\frac{t}{\sqrt{2}}(1-1j), \frac{t}{\sqrt{2}}(-1+1j)\}$, then for any random values of ζ_1 and ζ_2 we obtain $u = |t|$, where $t \in \mathbb{R}^+$, and \mathbb{R}^+ is the set of all positive real numbers.

Let $L_m^{\text{RIS}} = L_m^{\text{RISh}} L_m^{\text{RISg}}$, $\bar{\Phi}_i^{(n)} = \Phi_i^{(n)} - \phi_{i,m}^{(n)} - \psi^{(n)}$, and $\bar{\Phi}_m^{(n)} = \Phi_m^{(n)} - \phi_{m,m}^{(n)} - \psi^{(n)}$, thus, (8) and (9) can be expanded to:

$$A_m = \left| e^{j\theta_{M_1}} \sqrt{L_m^{\text{RIS}}} \sum_{n=1}^{N_m} \beta_{m,m}^{(n)} e^{j\bar{\Phi}_m^{(n)}} \right|^2, \quad (10)$$

$$I_m = \left| e^{j\theta_{M_1}} \left[\sqrt{L_m^{\text{RIS}}} \sum_{i \neq m}^{M_2-1} \left[\sum_{n=1}^{N_i} \beta_{i,m}^{(n)} e^{j\bar{\Phi}_i^{(n)}} \right] + v_m \right] \right|^2, \quad (11)$$

by considering (6), $\bar{\Phi}_m^{(n)}$ can be simplified to $\bar{\Phi}_m^{(n)} = \theta_m - \theta_{M_1}$, and thus, in (10), $e^{j\theta_{M_1}} e^{j\bar{\Phi}_m^{(n)}} = e^{j\theta_m}$, $\forall n$. Consequently, (10) and (11) can be re-expressed as

$$A_m = \left(\sqrt{L_m^{\text{RIS}}} \sum_{n=1}^{N_m} \beta_{m,m}^{(n)} \right)^2, \quad (12)$$

$$I_m = |I_{\text{RIS}} + v_m|^2, \quad (13)$$

where I_{RIS} is given by

$$I_{\text{RIS}} = \sqrt{L_m^{\text{RIS}}} \sum_{i \neq m}^{M_2-1} \left[\sum_{n=1}^{N_i} \beta_{i,m}^{(n)} e^{j\bar{\Phi}_i^{(n)}} \right] \quad (14)$$

By considering (12) and (13), (7) can be re-expressed as

$$\text{SINR}_m = \frac{A_m}{I_m + \frac{1}{\rho}}, \quad (15)$$

from (15), the instantaneous transmission rate for $U_{m,2}$ can be calculated as follows:

$$R_m = \log_2(1 + \text{SINR}_m), \quad (16)$$

and the sum-rate for the all M_2 users can be obtained as

$$R = \sum_{m=1}^{M_2} R_m = \sum_{m=1}^{M_2} \log_2(1 + \text{SINR}_m). \quad (17)$$

In the following section we derive the outage probability for a given user m in C_2 .

III. OUTAGE PROBABILITY ANALYSIS

Denoting the data rate requirement for $U_{m,2}$ as γ_m^* , the outage probability for $U_{m,2}$ is given as [30]

$$P_m^{\text{out}} = P(R_m < \gamma_m^*), \quad (18)$$

by substituting (16) in (18), we obtain

$$\begin{aligned} P_m^{\text{out}} &= P(\log_2(1 + \text{SINR}_m) < \gamma_m^*) \\ &= P\left(A_m - \bar{I}_m - \frac{2\gamma_m^* - 1}{\rho} < 0\right) \\ &= P(Y < y) \end{aligned} \quad (19)$$

where $Y = A_m - \bar{I}_m$, $y = \frac{2\gamma_m^* - 1}{\rho}$, and \bar{I}_m is given by

$$\bar{I}_m = (2\gamma_m^* - 1)I_m = |\sqrt{(2\gamma_m^* - 1)}(I_{\text{RIS}} + v_m)|^2. \quad (20)$$

From (19), we note that the outage probability is equivalent to the cumulative distribution function (CDF) of Y . In order to find the CDF of Y , we first find the distribution of the random variables (RVs) A_m and \bar{I}_m , as follows. By considering (12), we note that $\beta_{m,m}^{(n)}$ is a Rayleigh distributed RV with a mean $E[\beta_{m,m}^{(n)}] = \sqrt{\pi}/2$, and a variance $\text{VAR}[\beta_{m,m}^{(n)}] = (4 - \pi)/4$. According to the central limit theorem (CLT), for $N_m \gg 1$, the term inside the squared parenthesis is a Gaussian RV, $\sim \mathcal{N}(\sqrt{L_m^{\text{RIS}}} N_m \frac{\sqrt{\pi}}{2}, L_m^{\text{RIS}} N_m \frac{4 - \pi}{4})$. Thus, A_m is a non-central chi-square (χ^2) RV with one degree of freedom. Likewise, by considering (14), for $N - N_m \gg 1$, I_{RIS} is a Gaussian RV, $I_{\text{RIS}} \sim \mathcal{CN}(0, L_m^{\text{RIS}}(N - N_m))$. Consequently, the constant-scaled sum of the two independent Gaussian RVs in (20), $\sqrt{(2\gamma_m^* - 1)}(I_{\text{RIS}} + v_m)$, is a Gaussian RV, $\sim \mathcal{CN}(0, (2\gamma_m^* - 1)(L_m^{\text{RIS}}(N - N_m) + L_m^{\text{BS}}))$. Thus, \bar{I}_m is a central χ^2 RV with two degrees of freedom, and consequently, Y is the difference of a non-central and central independent χ^2 RVs, where its CDF is given by [31]

$$\begin{aligned} P_m^{\text{out}} &= 1 - \mathcal{Q}_{\frac{1}{2}}\left(\frac{\mu_1}{\sigma_1}, \sqrt{\frac{y}{s_1^2}}\right) + \left(\frac{s_2^2}{s_1^2 + s_2^2}\right)^{\frac{1}{2}} \exp\left(\frac{y}{2s_2^2}\right) \\ &\quad \times \exp\left(-\frac{\mu_1^2}{2(s_1^2 + s_2^2)}\right) \mathcal{Q}_{\frac{1}{2}}\left(\frac{\mu_1}{\sigma_1} \sqrt{\frac{s_2^2}{s_1^2 + s_2^2}}, \sqrt{\frac{y(s_1^2 + s_2^2)}{s_1^2 s_2^2}}\right) \end{aligned} \quad (21)$$

where \mathcal{Q}_k is the k^{th} order generalized Marcum Q-function [32], $\mu_1 = \sqrt{L_m^{\text{RIS}}} N_m \frac{\sqrt{\pi}}{2}$, $s_1^2 = L_m^{\text{RIS}} N_m \frac{4 - \pi}{4}$, and $s_2^2 = 0.5(2\gamma_m^* - 1)(L_m^{\text{RIS}}(N - N_m) + L_m^{\text{BS}})$. The asymptotic behaviour of the outage probability can be obtained when $\rho \rightarrow \infty$ or $y \rightarrow 0$, as follows:

$$\begin{aligned} P_m^{\infty} &= \lim_{\rho \rightarrow \infty} P_m^{\text{out}} = \lim_{y \rightarrow 0} P_m^{\text{out}} \\ &= 1 - \mathcal{Q}_{\frac{1}{2}}\left(\frac{\mu_1}{\sigma_1}, 0\right) + \left(\frac{s_2^2}{s_1^2 + s_2^2}\right)^{\frac{1}{2}} \exp\left(-\frac{\mu_1^2}{2(s_1^2 + s_2^2)}\right) \\ &\quad \times \mathcal{Q}_{\frac{1}{2}}\left(\frac{\mu_1}{\sigma_1} \sqrt{\frac{s_2^2}{s_1^2 + s_2^2}}, 0\right) \\ &= \left(\frac{s_2^2}{s_1^2 + s_2^2}\right)^{\frac{1}{2}} \exp\left(-\frac{\mu_1^2}{2(s_1^2 + s_2^2)}\right). \end{aligned} \quad (22)$$

From (22), it can be seen that the outage probability asymptotic performance is determined by the ratio of the RIS

elements allocated for a specific user to the RIS total size plus the strength of the BS interference link.

IV. RIS PARTITIONING APPROACH AND SPECIAL CASES

In this section, we provide the approach we used to partition the RIS among C_2 users in order to maximize user fairness. Since each sub-surface of the RIS is allocated to serve a different user, each user m in C_2 receives a significant interference from the other sub-surfaces allocated to the other users. Therefore, a proper number of reflecting elements (N_m) needs to be allocated for each user in order to guarantee the maximum fairness among them. In order to achieve this goal, we formulate an optimization problem where the Jain's fairness index [33] is the objective function to be maximized and $N_1, \dots, N_m, \dots, N_{M_2}$ are the decision variables to be determined, as follows:

$$(P1) : \max_{N_1, \dots, N_m, \dots, N_{M_2}} \frac{(\frac{1}{M_2} \sum_{m=1}^{M_2} \bar{R}_m)^2}{\frac{1}{M_2} \sum_{m=1}^{M_2} \bar{R}_m^2}, \quad (24a)$$

$$\text{s.t. } \sum_{m=1}^{M_2} N_m = N, N_m \in \{1, 2, 3, \dots, N - (M_2 - 1)\}, \forall m, \quad (24b)$$

where $\bar{R}_m = \mathbb{E}[R_m]$ is the ergodic rate of $U_{m,2}$, $\mathbb{E}[\cdot]$ is the statistical expectation operator over all the random channel realizations.

(P1) is NLIP problem with a non-convex feasible set represented by the constraint (24b) that has combinatorial growth as N increases. This makes (P1) a non-convex combinatorial optimization problem which is very challenging to solve if we consider the fact that a LIP is generally a non-deterministic polynomial-time (NP) hard problem [34]. IP optimization problems are usually solved by using branch-and-bound with the relaxation of the integrality constraint on the decision variables [35], which is, in this case, invalid for N_m , the number of RIS elements allocated to $U_{m,2}$. On the other hand, considering the exhaustive search solution, the complexity lies in the explosively large size of the feasible set represented by the constraint (24b) which has $\binom{N-1}{M_2-1}$ feasible points. This implies that the required searching loops to scan all the feasible points are at a complexity level of $\mathcal{O}((N-1)^{\min(M_2-1, N-M_2)})$, or $\mathcal{O}((N-1)^{M_2-1})$ if we consider the fact that $N \gg M_2$. Nevertheless, in order to shrink the size of the feasible set and thus, make the exhaustive search a practical method to solve (P1), we exploit the structure of the problem, specifically the nature of the transmission over the RIS, to bound the feasible set in (24b), as follows.

First, the number of RIS elements (N_m) allocated to any user m in C_2 cannot be randomly small, otherwise, the irremovable interference power from the other sub-surfaces overwhelms the amplification power from the m^{th} sub-surface. Motivated by the so-called interference temperature [36], a signal-to-interference power constraint (SIPC) [26] needs to be considered to protect each user $U_{m,2}$ from the interference belong to the other users. Based on the SIPC threshold, there is a minimum number of RIS elements N_{thr} that can be allocated

for any user m in C_2 to protect it from the interference power associated with the remaining part of the RIS ($N - N_{thr}$). This means that the feasible set in (24b) needs to have N_{thr} (rather than unity) as the minimum element in the set, which in turn shrinks the size of the feasible set to $\binom{N-N_{thr}-1}{M_2-1}$ feasible points. Second, instead of considering a step size of one between any two successive elements in the feasible set of (24b), an adjustable step size b is considered, which reduces the feasible set further to $\binom{\frac{N-N_{thr}}{b}-1}{M_2-1}$ feasible points, where $\frac{N-N_{thr}}{b}$ needs to be integer. Third, as in the power allocation of classical PD-NOMA, more RIS elements need to be allocated to the user with the weakest RIS- $U_{m,2}$ channel gain. Hence, the users need to be ordered according to their distances from the RIS, where $U_{m,2}$ is the m^{th} farthest user from the RIS and thus, the user with the m^{th} weakest RIS- $U_{m,2}$ channel gain. By considering the previously mentioned three bounding modifications on the feasible set in (24b), (P1) can be reformulated to obtain the following new optimization problem:

$$(P1.1) : \max_{N_1, \dots, N_m, \dots, N_{M_2}} \frac{(\frac{1}{M_2} \sum_{m=1}^{M_2} \bar{R}_m)^2}{\frac{1}{M_2} \sum_{m=1}^{M_2} \bar{R}_m^2}, \quad (25a)$$

$$\text{s.t. } \sum_{m=1}^{M_2} N_m = N, N_m \in \mathcal{N}, \forall m, \text{ where } \mathcal{N} = \{N_{thr}, N_{thr} + 1b, N_{thr} + 2b, \dots, N - N_{thr}(M_2 - 1)\}, \mathcal{N} \subset \mathbb{Z}^+, \quad (25b)$$

$$N_1 \geq N_2 \dots \geq N_{M_2}, \quad (25c)$$

where \mathbb{Z}^+ is the set of all positive integers. By considering (P1.1), it can be observed that the combinatorial growth of the feasible set of (P1) is significantly limited by the three modifications considered on the constraint (24b), which in turn effectively reduces the search space. In what follows, we formulate two new optimization problems to find the proper N_{thr} and b for (P1.1):

$$(P1.1.1) : \min N_{thr}, \quad (26a)$$

$$\text{s.t. } P(A_m | N_m = N_{thr} \leq q | I_{RIS} |_{M_2=2, i \neq m}|^2) \leq \epsilon \quad (26b)$$

$$M_2 N_{thr} \leq N. \quad (26c)$$

Here, the motivation behind the constraint (26b) can be explained by the fact that, from each user $U_{m,2}$ perspective, the RIS appears to be partitioned into two parts, the first part (with N_{thr} elements) that amplifies the signal of $U_{m,2}$, and the second part (with $N - N_{thr}$ elements) where the interference, associated with the other users, comes from. Thus, regardless of the noise and the BS- $U_{m,2}$ interference, the constraint (26b) ensures that for any user $U_{m,2}$ with N_{thr} RIS elements allocation, there is a low probability $\epsilon \ll 1$ that the interference power associated with the $N - N_{thr}$ part can be higher (by a factor of q) than the amplification power associated with the N_{thr} part. The two parameters ϵ and q need to be adjusted according to the size of the RIS and the number of users in C_2 . Furthermore, the probability given in (26b) can be obtained from (22) by following the same derivation steps provided in Section III and omitting the BS- $U_{m,2}$ interference term, as it is illustrated in Algorithm 1. The

constraint (26c) ensures that for a given N , N_{thr} needs to have a small enough value such that all the M_2 users can have (at least) the same allocation of N_{thr} RIS elements, otherwise, N need to be increased. In what follows we formulate an optimization problem to find the proper step size b for (P1.1).

$$(P1.1.2) : \quad \max \quad b, \quad (27a)$$

$$\text{s.t.} \quad \bar{R}_m^{(N_{thr}+b)} - \bar{R}_m^{(N_{thr})} \leq \bar{r}, \quad (27b)$$

$$b \leq N - M_2 N_{thr}, \quad (27c)$$

where $\bar{R}_m^{(N_{thr}+b)}$ and $\bar{R}_m^{(N_{thr})}$ are given as

$$\bar{R}_m^{(N_{thr}+b)} = \log_2 \left(1 + \frac{A_m |N_m=N_{thr}+b|}{|I_{RIS}|_{N_i=N-N_{thr}-b}|^2} \right), \quad (28)$$

$$\bar{R}_m^{(N_{thr})} = \log_2 \left(1 + \frac{A_m |N_m=N_{thr}|}{|I_{RIS}|_{N_i=N-N_{thr}}|^2} \right). \quad (29)$$

After determining N_{thr} in (P1.1.1), in (P1.1.2) we aim to find the maximum increment b that can be added to N_{thr} to get, accordingly, an ergodic rate increment upper-bounded by \bar{r} b/s/Hz. Thus, b corresponds to the step size of the exhaustive search that ensures a maximum of \bar{r} ergodic-rate resolution. In (27b), due to the fact that the users in C_2 experiences different SNR values and different BS- $U_{m,2}$ interference power levels, the ergodic rate difference is calculated in the absence of the noise and the BS- $U_{m,2}$ interference effects. In this way, b determined from (P1.1.2) ensures that in the presence of noise and BS- $U_{m,2}$ interference, the search resolution to solve (P1.1) does not exceed \bar{r} , for all users. Hence, \bar{r} needs to be adjusted according to the RIS size and number of users in C_2 .

A. RIS Partitioning Algorithms

Algorithms 1, 2 and 3 need to be applied in order, where Algorithm 1 is used first to obtain N_{thr} , which is the input of Algorithm 2. In the same way, Algorithm 2 is used to obtain b , then, N_{thr} and b are used as inputs to Algorithm 3, which can be summarized as follows. First, the set \mathcal{S} is constructed according to the constraints (25b) and (25c). The elements of \mathcal{S} are the possible splits the RIS can be partitioned into. When $b = 1$ is used in (25b), \mathcal{S} contains all the possible partitions and the solution of the algorithm is a global optimal solution, otherwise, for $b > 1$, the solution is a sub-optimal one. Second, for each split s in \mathcal{S} , the ergodic transmission rate \bar{R}_m for the all M_2 users are calculated and stored in the set $\mathcal{R}^{(s)}$. Third, for each partition s , Jain's index is calculated from $\mathcal{R}^{(s)}$ and stored in the set \mathcal{J} . Finally, the split j^* associated with the maximum Jain's index is chosen as the optimum split, and the set $\mathcal{S}^{(j^*)}$ contains the optimum number of RIS elements N_m^* needs to be allocated to each user m in C_2 .

B. Special Cases with Different Number of Users in Clusters

Here, in addition to the general case introduced in Section II, we consider the system performance analysis for particular cases in order to shed some light on the performance of the proposed scheme under different settings, as follows.

i) *All users are located in C_2* : In this scenario $M_1 = 0$, and the same transmission mechanism described in Section II is used here with the following single modification. Since there are no users in C_1 , the BS is assumed to transmit $x = \sqrt{P}\bar{x}$,

Algorithm 1 Solves (P1.1.1) to find N_{thr} .

Require: L_m^{RIS} , M_2 , N , q , ϵ .

1: Initialize $N_{thr} = 1, m = 1, i = 2$.

2: **repeat**

3: $\mu_m = \sqrt{L_m^{\text{RIS}} N_{thr} \frac{\sqrt{\pi}}{2}}, s_m^2 = L_m^{\text{RIS}} N_{thr} \frac{4-\pi}{4}, s_i^2 = 0.5 L_m^{\text{RIS}} q (N - N_{thr})$.

4: The probability in (22b) can be obtained from (22):

$$P_m^\infty = \left(\frac{s_i^2}{s_m^2 + s_i^2} \right)^{\frac{1}{2}} \exp \left(-\frac{\mu_m^2}{2(s_m^2 + s_i^2)} \right).$$

5: $N_{thr} = N_{thr} + 1$.

6: **while** $P_m^\infty \leq \epsilon$ and $M_2 N_{thr} \leq N$.

7: **return** $N_{thr} = N_{thr} - 1$.

Algorithm 2 Solves (P1.1.2) to find the step size b .

Require: N , N_{thr} , \bar{r} , $\beta_{m,m}^{(n)}$, $\beta_{i,m}^{(n)}$, Φ_i^n , $\forall n$, and for any m and i such that $i \neq m$.

1: Initialize $b = 1$.

2: $\bar{R}_m^{(N_{thr})} = \mathbb{E} \left[\log_2 \left(1 + \frac{A_m |N_m=N_{thr}|}{|I_{RIS}|^2} \right) \right]$. Perform the expectation over 10^5 random channel realizations [37].

3: **repeat**

4: $\bar{R}_m^{(N_{thr}+b)} = \mathbb{E} \left[\log_2 \left(1 + \frac{A_m |N_m=N_{thr}+b|}{|I_{RIS}|^2} \right) \right]$. Perform the expectation over 10^5 random channel realizations.

5: $\bar{r}_{diff} = \bar{R}_m^{(N_{thr}+b)} - \bar{R}_m^{(N_{thr})}$.

6: $b = b + 1$.

7: **while** $\bar{r}_{diff} \leq \bar{r}$ and $b \leq N - M_2 N_{thr}$.

8: **return** $b = b - 1$.

where \bar{x} is a predetermined symbol. Thus, assuming v_m is known at the receiver side, the signal $v_m \bar{x}$ received by each user m in C_2 over the BS- $U_{m,2}$ link can be removed readily. Furthermore, over the RIS- $U_{m,2}$ link, each sub-surface of the RIS rotates \bar{x} to reflect the PSK symbol to be transmitted to $U_{m,2}$, as described in Section II. Without loss of generality, an unmodulated carrier signal can be sent from the BS and, in this case, the BS can be compensated by a single RF signal generator (SG), which simplifies the transmitter architecture. Note that when the mutual sub-surfaces interference power is significantly larger than the noise power, for all users in C_2 , the uniform allocation of the RIS elements ($N_m = \frac{N}{M_2}, \forall m$) guarantees the maximum fairness between these users. Furthermore, the instantaneous transmission rate of $U_{m,2}$ can be obtained from (16) by substituting $v_m = 0$, as follows:

$$R_m = \log_2 \left(1 + \frac{A_m}{I_m |v_m=0 + \frac{1}{\rho}} \right). \quad (30)$$

In order to obtain the outage probability of $U_{m,2}$, the same derivation steps provided in Section III are followed here. The outage probability of $U_{m,2}$ for a targeted γ_m^* can be obtained from (21) with the following single modification. By considering $I_m |v_m=0$, we get $s_2^2 = 0.5 L_m^{\text{RIS}} (2^{\gamma_m^*} - 1) (N - N_m)$, while s_1^2 , y , μ_1 remain unchanged. Furthermore, the asymptotic behaviour of the outage probability can be obtained from (22) with previously mentioned modification.

ii) *Each cluster has a single user*: In this scenario, $U_{1,1}$ and $U_{1,2}$ are the only users in C_1 and C_2 , respectively. Therefore, the BS transmits $x = \sqrt{P}x_1$, and $U_{1,1}$ experience the same

Algorithm 3 RIS partitioning algorithm to solve (P1.1)

Require: b , N_{thr} , N , M_2 , L_m^{RIS} , ρ , v_m , $\beta_{i,m}^{(n)}$, $\phi_{i,m}^{(n)}$, $\bar{\Phi}_i^n$, $\forall i, n, m$.

- 1: Construct the set \mathcal{N} in the constraint (25b). Choose $b = 1$ or $b > 1$ (from Algorithm 2) for the optimal and sub-optimal solutions, respectively.
- 2: According to the constraint (25b), construct the set \mathcal{S} by finding all the solutions of $\sum_{m=1}^{M_2} N_m = N$, where $N_m \in \mathcal{N}$, and excluding the ones that do not satisfy (25c). Thus, $\mathcal{S} = \{\tilde{\mathcal{S}}^{(1)}, \dots, \tilde{\mathcal{S}}^{(s)}, \dots, \tilde{\mathcal{S}}^{(|\mathcal{S}|)}\}$, where $|\mathcal{S}|$ is the cardinality of the set \mathcal{S} and $\tilde{\mathcal{S}}^{(s)} = \{N_1^{(s)}, \dots, N_m^{(s)}, \dots, N_M^{(s)}\}$ corresponds to the RIS split s , $\tilde{\mathcal{S}}^{(s)} \subset \mathcal{N}$, $\forall s$.
- 3: Construct the new sets $\mathcal{R}^{(1)}, \dots, \mathcal{R}^{(s)}, \dots, \mathcal{R}^{(|\mathcal{S}|)}$, where $\mathcal{R}^{(s)} = \{\emptyset\}$, $\forall s$.
- 4: **for** $s = 1 : |\mathcal{S}|$ **do**
- 5: **for** $m = 1 : M_2$ **do**
- 6: $R_m = \mathbb{E} \left[\log_2 \left(1 + \frac{A_m}{I_m + \frac{1}{\rho}} \right) \right]$, where N_i , $N_m \in \tilde{\mathcal{S}}^{(s)}$, $\forall i, m$. Perform the expectation over 10^5 random channel realizations.
- 7: $\mathcal{R}^{(s)} = \mathcal{R}^{(s)} \cup \{R_m\}$.
- 8: **end for**
- 9: **end for**
- 10: Construct a new set $\mathcal{J} = \{\emptyset\}$.
- 11: **for** $s = 1 : |\mathcal{S}|$ **do**
- 12: $J = \frac{(\frac{1}{M_2} \sum_{m=1}^{M_2} R_m)^2}{\frac{1}{M_2} \sum_{m=1}^{M_2} R_m^2}$, where $R_m \in \mathcal{R}^{(s)}$, $\forall m$.
- 13: $\mathcal{J} = \mathcal{J} \cup \{J\}$.
- 14: **end for**
- 15: $j^* = \arg \max_{j=1:|\mathcal{J}|} \mathcal{J}^{(j)}$
- 16: **return** $\tilde{\mathcal{S}}^{(j^*)} = \{N_1^*, N_2^*, \dots, N_m^*, \dots, N_{M_2}^*\}$.

performance in a SISO system. On the other hand, the RIS rotate x and reflects the PSK symbol to be transmitted to $U_{1,2}$, as described in Section II. Since the whole surface is allocated for $U_{1,2}$, its instantaneous transmission rate can be obtained from (16) by omitting the sub-surfaces interference term, as follows:

$$R_1 = \log_2 \left(1 + \frac{A_1|_{N_1=N}}{I_1|_{I_{RIS}=0} + \frac{1}{\rho}} \right). \quad (31)$$

By following the same derivation steps provided in Section III, we obtain the outage probability of $U_{1,2}$ for a targeted γ_1^* from (21), with the following modifications. $\mu_1 = \sqrt{L_1^{RIS} N \frac{\sqrt{\pi}}{2}}$, and $s_1^2 = L_1^{RIS} N \frac{4-\pi}{4}$. By considering $I_1|_{I_{RIS}=0}$, we get $s_2^2 = 0.5L_1^{BS}(2\gamma_1^* - 1)$, while y remain unchanged. Furthermore, the asymptotic behaviour of the outage probability can be obtained from (22) with the previously mentioned modifications.

V. SIMULATION RESULTS

In this section, we provide computer simulation results for the proposed scheme against the following three benchmark schemes: the time division multiple access (TDMA) as an OMA scheme, classical PD-NOMA scheme, and the RIS-assisted SISO NOMA scheme proposed in [10] [11]. For

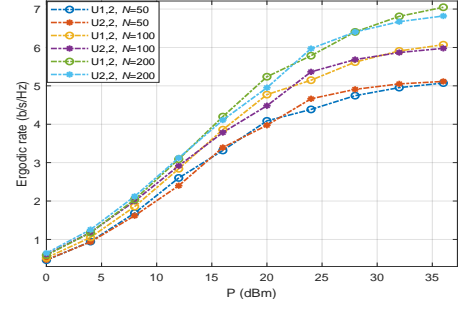


Fig. 2. The performance of the RIS partitioning algorithms with different N values.

TABLE I
USERS' DISTANCES FOR DIFFERENT DEPLOYMENT SCENARIOS.

Users' deployment	$d_{1,1}$, $r_{1,1}$	$d_{2,1}$, $r_{2,1}$	$d_{1,2}$, $r_{1,2}$	$d_{2,2}$, $r_{2,2}$
$M_1 = 0, M_2 = 2$	-	-	150, 146	100, 104
$M_1 = 1, M_2 = 1$	150, 146	-	100, 104	-
$M_1 = 2, M_2 = 2$	150, 154	100, 104	250, 254	200, 204

TABLE II
RIS PARTITIONING ALGORITHMS: INPUT PARAMETERS AND OUTCOMES.

N	N_{thr}, q, ϵ	b, \bar{r}	Number of splits: sub-opt/opt.
50	15, 1.5, 0.1	2, 0.3	5/49
100	21, 1.5, 0.1	5, 0.5	5/99
200	32, 1.5, 0.05	10, 0.7	6/199

TDMA and classical NOMA schemes, in order to achieve maximum user fairness, we optimize the time and power allocation at the transmitter side using exhaustive search. In order to guarantee a fair comparison, we consider the maximum fairness between users as the common threshold for all schemes, while the comparison lies in the ergodic transmission rates and outage probability performance. In what follows, we describe our path loss models and other simulation parameters.

For the BS- $U_{m,c}$ link, where c denotes the cluster number, we consider the following path loss model [38]:

$$(L_m^{BS})^{-1} = C_0 \left(\frac{d_{m,c}}{D_0} \right)^\alpha, \quad (32)$$

where $C_0 = -30$ dB is the path gain at the reference distance $D_0 = 1$ m, $d_{m,c}$ is the BS- $U_{m,c}$ distance, and $\alpha = -3.5$ is the path gain exponent.

For the BS-RIS- $U_{m,2}$ link, we consider that the RIS is located in the far-field with respect to the BS by ensuring that $r_s^1 \geq \frac{N\lambda}{2}$ [39], thus, the path loss is given by (with maximum gain RIS elements) [25]

$$(L_m^{RIS})^{-1} = \frac{\lambda^4}{256\pi^2 r_s^2 r_m^2}, \quad (33)$$

where r_s and r_m are the BS-RIS (the center point), and the RIS (the center point)- $U_{m,2}$ distances, all in meters. Due to the small spacing distances between the RIS elements

¹The considered N values are $N = 20, 26, 34, 40, 42, 50, 60, 80, 100$ and 200 RIS elements, therefore, the BS-RIS distance is adjusted to be $r_s = 3, 3, 3, 5, 5, 5, 6, 8, 9$ and 17 m, respectively.

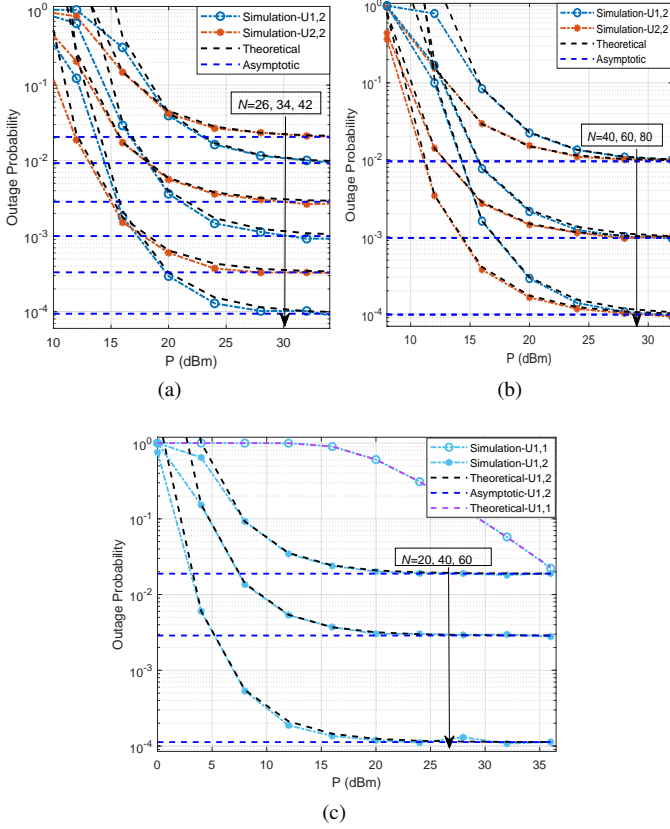


Fig. 3. Outage probability performance with different N values, for (a) the general case, $M_1 = 2$, $M_2 = 2$, and a targeted transmission rate of 0.75 bit per channel use (bpcu) for all users, (b) the first case, $M_1 = 0$, $M_2 = 2$, $\gamma_1^* = \gamma_2^* = 2$ bpcu, (c) the second case, $M_1 = 1$, $M_2 = 1$, and a targeted transmission rate of 2 bpcu for both users.

compared to r_s and r_m , we consider r_s and r_m for the path loss calculations, consequently, the path losses for all the RIS elements are considered the same. In Table I, we give the users' distances from the BS and RIS, for different deployment scenarios, which are the used distances in our simulations, unless stated otherwise. Furthermore, the noise power is assumed to be fixed and identical for all users in C_1 and C_2 , $\sigma^2 = -90$ dBm, $\forall m$, and the simulations are performed with 10^5 random channel realizations.

Fig. 2 illustrates the performance of the sub-optimal solution to (P1), which is represented by Algorithms 1, 2, and 3 to solve (P1.1) (the reformulated version of (P1)). Here, we consider that one user is located in C_1 and two users in C_2 ($M_1 = 1$, $M_2 = 2$) where the RIS needs to be partitioned among them. It can be seen that the proposed algorithms achieve a close result to the perfect user fairness between the two users with different N values. Furthermore, Table II shows that Algorithms 1 and 2 reduce the search space for Algorithm 3 significantly, which makes the exhaustive search a practical solution to find the proper RIS split.

Figs. 3 (a)-(c) show the outage probability performance for the general case, the first and second cases, respectively, with different N values, where the theoretical and simulation curves are in perfect agreement with each other. Note that, as the performance improves with the increase of N , the saturation happens at the high SNR region due to the interference coming

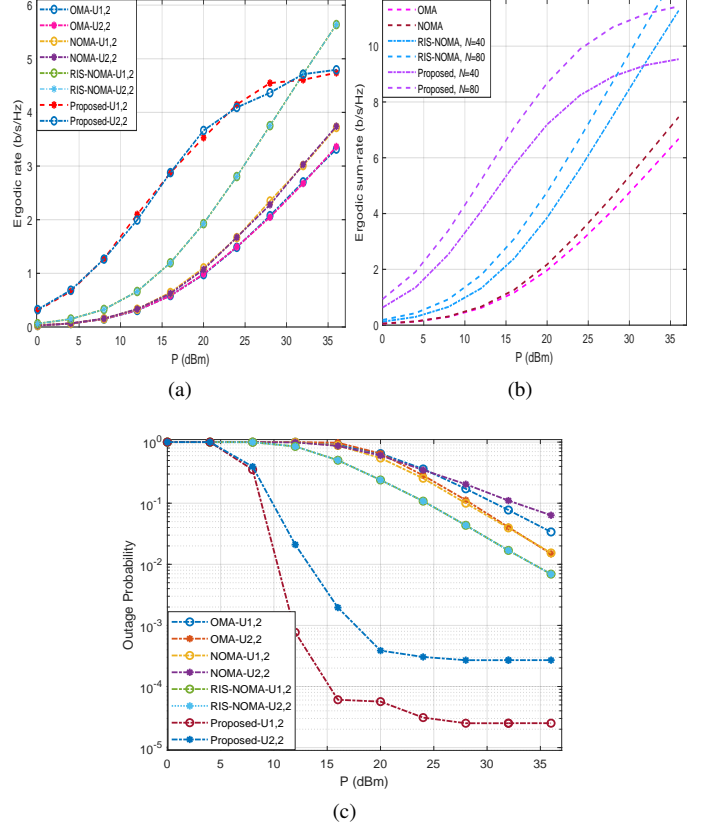


Fig. 4. The comparison of the proposed and benchmark schemes with $M_1 = 0$ and $M_2 = 2$, in terms of (a) ergodic rate with $N = 40$, (b) ergodic sum-rate with $N = 40$ and $N = 80$, (c) the outage probability, with a targeted transmission rate of 1.2 bpcu for all users, and $N = 40$.

from BS and/or sub-surfaces.

In what follows we compare the proposed scheme with different benchmark schemes by considering the two special cases introduced in Section IV-B and the general case introduced in Section II. Note that, due to the small values of M_1 , M_2 , and N the RIS partitioning for the proposed system is obtained directly from Algorithm 3 with $N_{thr} = 0$ and $b = 1$ for all three comparison cases. Furthermore, the RIS partitioning is performed for each P value to obtain the proper number of RIS elements that need to be allocated to each sub-surface.

In Figs. 4 (a)-(c), we consider the first case with $N = 40$, $M_1 = 0$, and $M_2 = 2$. As it is shown in Fig. 4 (a), all the schemes achieve almost the same user fairness, nevertheless, the proposed scheme shines out with an improvement in the required P of 8 dB compared to the RIS-NOMA scheme and 14 dB compared to TDMA-OMA and PD-NOMA schemes. However, the performance gain achieved by the proposed scheme is bounded by a saturation point due to the mutual sub-surfaces interference. Fig. 4 (b) shows the ergodic sum-rate comparison, where doubling the RIS size results in almost a 2 dB up to 14 dB improvement in the required P for the proposed scheme starting from the low to the high SNR region, respectively, while around 3 dB improvement is achieved by the RIS-NOMA scheme. This shows that the proposed scheme benefits from increasing the RIS size effectively more

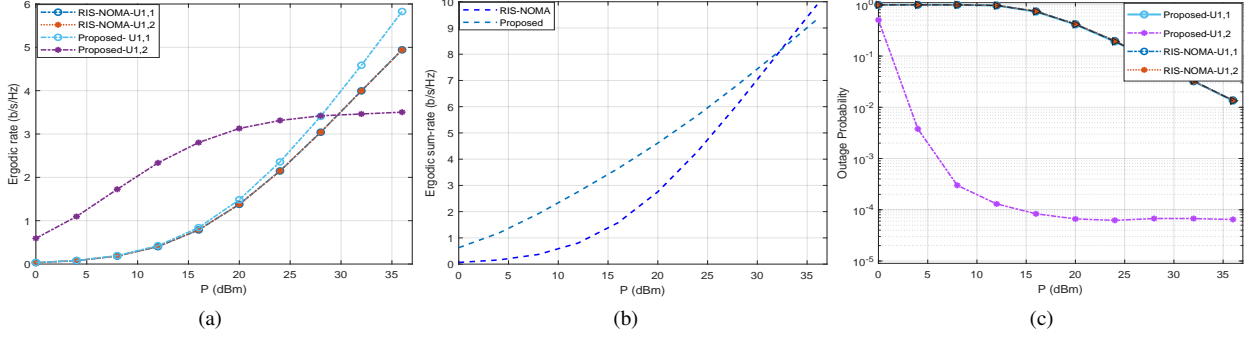


Fig. 5. The comparison of the proposed and the RIS-NOMA benchmark schemes with $M_1 = M_2 = 1$ and $N = 40$, in terms of (a) ergodic rate, (b) ergodic sum-rate, (c) outage probability, with a targeted transmission rate of 1.2 bpcu for all users.

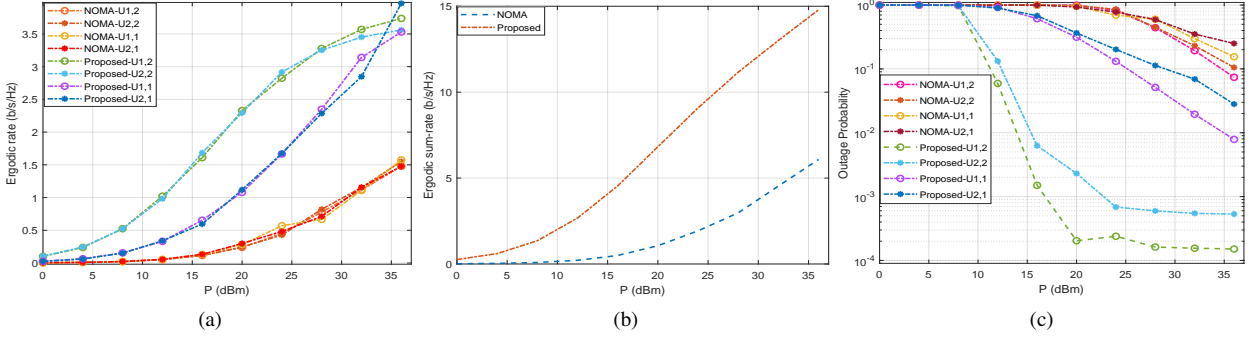


Fig. 6. The comparison of the proposed and the NOMA benchmark schemes with $M_1 = M_2 = 2$ and $N = 40$, in terms of (a) ergodic rate, (b) ergodic sum-rate, (c) outage probability, with a targeted transmission rate of 0.75 bpcu for all users.

compared to the RIS-NOMA scheme. Fig 4 (c) shows the outage probability comparison with a targeted transmission rate of 1.2 bpcu for all users. It can be seen that the proposed scheme outperforms the benchmark schemes with a around 20 dB in the required P for both users before the saturation region.

In Figs. 5 (a)-(c), we consider the second case with $N = 40$ and $M_1 = M_2 = 1$, as follows. Fig. 5 (a) shows that $U_{1,1}$ in the proposed scheme and $U_{1,1}$ and $U_{1,2}$ in the RIS-NOMA scheme, achieve almost the same ergodic rate performance, with a 2 dB improvement in the required P for the proposed scheme at the high SNR region. On the other hand, $U_{1,2}$ in the proposed scheme achieves a 12 dB improvement compared to the other users, which can be explained by the asymptotic squared power gain of $\mathcal{O}(N^2)$ the RIS provides to $U_{1,2}$ [38]. However, there is a saturation point for the performance of $U_{1,2}$ due to the BS- $U_{1,2}$ interference link. Considering the user fairness, contrary to might be concluded for the first glance from Fig. 5 (a), the proposed scheme achieves the maximum user fairness, which can be explained as follows. Since the communication link over the RIS is blocked for $U_{1,1}$ in both schemes, the most efficient option, in terms of the sum-rate performance and user fairness, is to fully allocate the RIS to serve $U_{1,2}$ and the BS to serve $U_{1,1}$ in both schemes, which is what the proposed scheme basically does. On the other hand, the use of SC in the benchmark scheme makes the RIS amplifies the interference from $U_{1,1}$ to $U_{1,2}$ without any benefit for $U_{1,1}$, which is unfair to $U_{1,2}$. In Fig. 5 (b), compared to the RIS-NOMA scheme, the

ergodic sum-rate of the proposed scheme achieves a maximum of 8 dB improvement in the required P at the low SNR region, however, this gain decreases as the SNR increases until 33 dB, where the RIS-NOMA starts to outperform the proposed scheme. In Fig. 5 (c), $U_{1,2}$ in the proposed scheme outperforms the other users in both schemes with a remarkable improvement of 31 dB in the required P , while the other users achieve the same performance, which agrees with the ergodic rate results shown in Fig. 5 (a).

Finally, in Figs. 6 (a)-(c), we consider the general case of four users, $M_1 = M_2 = 2$ and $N = 40$, for the proposed and NOMA schemes. Fig. 6 (a) shows the ergodic rate performance for all users, where almost maximum user fairness is achieved by the NOMA scheme. On the other hand, the proposed scheme provides a close to the maximum fairness performance between the two users in each cluster, which is corresponds to the maximum fairness between all the four users due to the same reasons explained in the discussion of Fig. 5 (a). Furthermore, the performance of the proposed scheme outperforms the one of NOMA scheme for each user significantly, with more than 12 dB and 20 dB improvement for the two users in C_1 and the two users in C_2 , respectively. Overall, for the ergodic sum-rate there is an improvement of 15 dB achieved by the proposed scheme compared to the NOMA scheme, as shown in Fig. 6 (b). In Fig. 6 (c), the proposed scheme outperforms NOMA scheme in the outage probability performance with around 22 dB in the required P for the first and second users in C_2 , and around 5 dB and 10 dB for the first and second users in C_1 , respectively.

VI. CONCLUSION

In this paper, we have introduced a novel downlink NOMA solution with RIS partitioning. In the proposed system, the ergodic rates and outage probabilities of all users are enhanced and the user fairness is maximized by the fair and efficient distribution of the physical resources (BS and RIS) among users. Furthermore, we have proposed three efficient searching algorithms to, sequentially, obtain a sub-optimal solution for the RIS partitioning optimization problem, with insignificant performance degradation. In addition to the general case, we have provided two special cases to provide an insight into the performance of the proposed system in different environment settings. We have derived the exact and asymptotic outage probability expressions for the proposed system in all the cases. The proposed system is compared with three benchmark systems namely, TDMA, classical NOMA, and an RIS-assisted NOMA system. The computer simulations show that the proposed system outperforms the benchmark systems significantly, in terms of outage probability, ergodic rates of all users, and user fairness. On the other hand, the proposed system simplifies the detection process for C_1 users by reducing the number of the required SIC iterations, and for C_2 users by totally obviating the need for SIC technique.

REFERENCES

- [1] Y. Saito *et al.*, "Non-orthogonal multiple access (NOMA) for cellular future radio access," in *2013 IEEE 77th Veh. Technol. Conf. (VTC Spring)*, June 2013, pp. 1–5.
- [2] S. M. R. Islam, N. Avazov, O. A. Dobre, and K. Kwak, "Power-domain non-orthogonal multiple access (NOMA) in 5G systems: Potentials and challenges," *IEEE Commun. Surveys Tuts.*, vol. 19, no. 2, pp. 721–742, Oct. 2017.
- [3] Z. Ding, Z. Yang, P. Fan, and H. V. Poor, "On the performance of non-orthogonal multiple access in 5G systems with randomly deployed users," *IEEE Signal Processing Lett.*, vol. 21, no. 12, pp. 1501–1505, Jul. 2014.
- [4] X. Yue, Z. Qin, Y. Liu, S. Kang, and Y. Chen, "A unified framework for non-orthogonal multiple access," *IEEE Trans. Commun.*, vol. 66, no. 11, pp. 5346–5359, May 2018.
- [5] E. Basar *et al.*, "Wireless communications through reconfigurable intelligent surfaces," *IEEE Access*, vol. 7, pp. 116753–116773, Aug. 2019.
- [6] Q. Wu and R. Zhang, "Towards smart and reconfigurable environment: Intelligent reflecting surface aided wireless network," *IEEE Commun. Mag.*, vol. 58, no. 1, pp. 106–112, Nov. 2019.
- [7] E. Basar, "Transmission through large intelligent surfaces: A new frontier in wireless communications," in *2019 European Conf. Netw. Commun. (EuCNC)*, June. 2019, pp. 112–117.
- [8] —, "Reconfigurable intelligent surface-based index modulation: A new beyond MIMO paradigm for 6G," *IEEE Trans. Commun.*, vol. 68, no. 5, pp. 3187–3196, Feb. 2020.
- [9] A. Khaleel and E. Basar, "Reconfigurable intelligent surface-empowered MIMO systems," *IEEE Systems Journal*, pp. 1–9, Aug. 2020.
- [10] G. Yang, X. Xu, Y.-C. Liang, "Intelligent reflecting surface assisted non-orthogonal multiple access," Dec. 2019. [Online]. Available: arXiv:1907.03133.
- [11] G. Yang, X. Xu, and Y.-C. Liang, "Intelligent reflecting surface assisted non-orthogonal multiple access," in *2020 IEEE Wireless Commun. Netw. Conf. (WCNC)*, May 2020, pp. 1–6.
- [12] Z. Ding and H. Vincent Poor, "A simple design of IRS-NOMA transmission," *IEEE Commun. Lett.*, vol. 24, no. 5, pp. 1119–1123, Feb. 2020.
- [13] T. Hou *et al.*, "Reconfigurable intelligent surface aided NOMA networks," *IEEE J. Sel. Areas in Commun.*, vol. 38, no. 11, pp. 2575–2588, Jul. 2020.
- [14] M. Zhang, M. Chen, Z. Yang, H. Asgari, and M. Shikh-Bahaei, "Joint user clustering and passive beamforming for downlink NOMA system with reconfigurable intelligent surface," in *2020 IEEE 31st Annual Int. Symposium on Personal, Indoor and Mobile Radio Commun.*, Aug. 2020, pp. 1–6.
- [15] Y. Xu *et al.*, "Fair non-orthogonal multiple access communication systems with reconfigurable intelligent surface," in *2020 IEEE 31st Annual Int. Symposium on Personal, Indoor and Mobile Radio Communications*, Aug. 2020, pp. 1–6.
- [16] X. Liu, Y. Liu, Y. Chen, and H. V. Poor, "RIS enhanced massive non-orthogonal multiple access networks: Deployment and passive beamforming design," *IEEE J. Sel. Areas Commun.*, pp. 1–1, Aug. 2020.
- [17] Y. Li, M. Jiang, Q. Zhang, and J. Qin, "Joint beamforming design in multi-cluster MISO NOMA reconfigurable intelligent surface-aided downlink communication networks," *IEEE Trans. Commun.*, pp. 1–1, Oct. 2020.
- [18] T. Hou, Y. Liu, Z. Song, X. Sun, and Y. Chen, "MIMO-NOMA networks relying on reconfigurable intelligent surface: A signal cancellation based design," *IEEE Trans. Commun.*, pp. 1–1, Aug. 2020.
- [19] C. Zhang, W. Yi, Y. Liu, "Reconfigurable intelligent surfaces aided multi-cell NOMA networks: A stochastic geometry model," Aug. 2020. [Online]. Available: arXiv:2008.08457.
- [20] C. Zhang, W. Yi, Y. Liu, Z. Qin, K.K. Chai, "Downlink analysis for reconfigurable intelligent surfaces aided NOMA networks," Jun. 2020. [Online]. Available: arXiv:2006.13260.
- [21] M. Elhattab, M. A. Arfaoui, C. Assi, and A. Ghayeb, "Reconfigurable intelligent surface assisted coordinated multipoint in downlink NOMA networks," *IEEE Commun. Lett.*, pp. 1–1, Oct. 2020.
- [22] Z. Ding, R. Schober, and H. V. Poor, "On the impact of phase shifting designs on IRS-NOMA," *IEEE Wireless Commun. Lett.*, vol. 9, no. 10, pp. 1596–1600, Apr. 2020.
- [23] J. Zuo, Y. Liu, Z. Qin, and N. Al-Dhahir, "Resource allocation in intelligent reflecting surface assisted NOMA systems," *IEEE Trans. Commun.*, pp. 1–1, Aug. 2020.
- [24] Q. Wu and R. Zhang, "Intelligent reflecting surface enhanced wireless network via joint active and passive beamforming," *IEEE Trans. Wireless Commun.*, vol. 18, no. 11, pp. 5394–5409, Aug. 2019.
- [25] S.W. Ellingson, "Path loss in reconfigurable intelligent surface-enabled channels," Dec. 2019. [Online]. Available: arXiv:1912.06759.
- [26] X. Kang, H. F. Chong, Y. Chia, and S. Sun, "Ergodic sum-rate maximization for fading cognitive multiple-access channels without successive interference cancellation," *IEEE Trans. Veh. Technol.*, vol. 64, no. 9, pp. 4009–4018, Oct. 2014.
- [27] T. Hou *et al.*, "Reconfigurable intelligent surface aided NOMA networks," *IEEE J. Sel. Areas Commun.*, vol. 38, no. 11, pp. 2575–2588, Jul. 2020.
- [28] W. Xia, Y. Zhou, G. Yang, and R. T. Chen, "Optimal minimum euclidean distance-based precoder for NOMA with finite-alphabet inputs," *IEEE Access*, vol. 7, pp. 45 123–45 136, Apr. 2019.
- [29] J. Zhang, X. Wang, T. Hasegawa, and T. Kubo, "Downlink non-orthogonal multiple access (NOMA) constellation rotation," in *2016 IEEE 84th Veh. Technol. Conf. (VTC-Fall)*, Sep. 2016, pp. 1–5.
- [30] J. G. Proakis, "Digital Communications," 5th ed. New York: McGrawHill, 2008.
- [31] M. Simon, "Probability Distributions Involving Gaussian Random Variables," New York, NY, USA: Springer, 2002.
- [32] A. Annamalai, C. Tellambura, and J. Matyas, "A new twist on the generalized marcum q-function $qm(a, b)$ with fractional-order m and its applications," in *2009 6th IEEE Consumer Commun. Netw. Conf.*, Jan. 2009, pp. 1–5.
- [33] R. Jain, D.-M. Chiu, W. R. Hawe, "A quantitative measure of fairness and discrimination for resource allocation in shared computer system," Eastern Research Laboratory, Digital Equipment Corporation Hudson, MA, 1984, vol. 38.
- [34] L. A. Wolsey and G. L. Nemhauser, *Integer and Combinatorial Optimization*. New York: John Wiley and Sons, 1988.
- [35] S. Burer and A. N. Letchford, "Non-convex mixed-integer nonlinear programming: A survey," *Surv. Oper. Res. Manage. Sci.*, vol. 17, no. 2, pp. 97–106, Jun. 2012.
- [36] S. Haykin, "Cognitive radio: Brain-empowered wireless communications," *IEEE J. Sel. Areas Commun.*, vol. 23, no. 2, pp. 201–220, Feb. 2005.
- [37] R. Zhang, S. Cui, and Y. Liang, "On ergodic sum capacity of fading cognitive multiple-access and broadcast channels," *IEEE Trans. Inf. Theory*, vol. 55, no. 11, pp. 5161–5178, Oct. 2009.
- [38] Q. Wu and R. Zhang, "Intelligent reflecting surface enhanced wireless network via joint active and passive beamforming," *IEEE Trans. Wireless Commun.*, vol. 18, no. 11, pp. 5394–5409, Aug. 2019.
- [39] W. Tang *et al.*, "Wireless communications with reconfigurable intelligent surface: Path loss modeling and experimental measurement," *IEEE Trans. Wireless Commun.*, pp. 1–1, Sep. 2020.